Bull. Mater. Sci., Vol. 40, No. 6, October 2017, pp. 1121–1125
DOI 10.1007/s12034-017-1477-y

High-pressure studies of superconductivity in $BiO_{0.75}F_{0.25}BiS_2$

ZEBA HAQUE[1], GOHIL S THAKUR[1,5], GANESAN KALAI SELVAN[2], SONACHALAM ARUMUGAM[2], L C GUPTA[1,4] and A K GANGULI[1,3,*]

[1]Department of Chemistry, Indian Institute of Technology Delhi, New Delhi 110016, India
[2]Centre for High Pressure Research, School of Physics, Bharathidasan University, Tiruchirappalli 620024, India
[3]Institute of Nano Science and Technology, Habitat Centre, Mohali, Punjab 160062, India
[4]Solid State and Nano Research Laboratory, Department of Chemistry, IIT Delhi, New Delhi 110016, India
[5]*Present address:* Max Planck Institute for Chemical Physics of Solids, Dresden 01189, Germany
*Author for correspondence (ashok@chemistry.iitd.ac.in)

MS received 15 September 2016; accepted 7 March 2017; published online 25 September 2017

Abstract. $BiO_{0.75}F_{0.25}BiS_2$ crystallizes in tetragonal $CeOBiS_2$ structure (S. G. $P4/nmm$). We have investigated the effect of pressure on magnetization measurements. Our studies suggest improved superconducting properties in polycrystalline samples of $BiO_{0.75}F_{0.25}BiS_2$. The T_c in our sample is 5.3 K, at ambient pressure, which is marginal but definite enhancement over T_c reported earlier (= 5.1 K). The upper critical field $H_{c2}(0)$ is greater than 3 T, which is higher than earlier report on this material. As determined from the M–H curve, both H_{c2} and H_{c1} decrease under external pressure P ($0 \leq P \leq 1$ GPa). We observe a decrease in critical current density and transition temperature on applying pressure in $BiO_{0.75}F_{0.25}BiS_2$.

Keywords. Superconductivity; crystal structure; resistivity; high pressure magnetism.

1. Introduction

Crystal structure of the parent $LnOBiS_2$ (Ln = La, Ce, Pr, Nd and Yb) consists of double BiS_2 layers stacked alternately with an Ln_2O_2 blocking layer. These semiconducting materials were made superconducting by doping F at the O-site or by introducing M^{4+} ions (M = Th, Hf, Zr and Ti) at the Ln^{3+}-site. This approach yielded materials with $T_c \sim 2.5$–10 K [1–8]. Taking clue from the rare-earth-based oxypnictides superconductors, LnO-layer was replaced by SrF-layer, thereby generating a new material $SrFBiS_2$ [9]. Superconductivity was induced in $SrFBiS_2$, $T_c \sim 2.7$–10 K, by doping it with Ln (Ln = La, Ce, Pr, Nd and Sm) at the Sr-site [10–12]. The parent phases, i.e., $LnOBiS_2$, $SrFBiS_2$ and $BiOBiS_2$, are known to be semiconducting [1,2,5,6,9,13]. $EuFBiS_2$, the Eu-analogue of $SrFBiS_2$, shows metallic conduction and becomes superconducting at 0.3 K without any doping. As a consequence of electron doping under ambient condition, $Eu_{1-x}Ln_xFBiS_2$ shows enhanced $T_c \sim 2.2$ K, and 10 K under pressure [14,15]. $LnO_{1-x}F_xBiS_2$ (Ln = La, Ce, Pr and Nd) [2,4,5,8] and $Sr_{1-x}La_xFBiS_2$ [9] show abrupt increase in T_c from ~2 to 10 K upon application of pressure [16–20]. The increase in T_c of $LaO_{0.5}F_{0.5}BiS_2$ is accompanied by a structural phase transition from a tetragonal to a monoclinic ($P21/m$) structure observed from high-pressure X-ray diffraction (XRD) measurements [18]. This enhancement of T_c could be related to the suppression of semiconducting behaviour in this material, which shows an increase in the density of charge carriers [16]. On the other hand $Bi_4O_4S_3$ exhibits $T_c = 4.5$ K at ambient pressure, and it shows a decrease in T_c down to 3 K upon applying pressure ~2 GPa [21]. Therefore, one can see the antagonistic pressure effects on the two classes of superconductors, i.e., on applying pressure the superconducting transition temperature T_c decreases for the one with metallic normal state resistivity and increases for the systems possessing semiconducting-type normal state resistivity.

In the $BiOBiS_2$ phase, the two Bi atoms occupy two different crystallographic positions. One of them is present in the blocking layer and the other goes to the conduction layer. Shao *et al* [13] studied the effect of F doping at O-sites in $BiOBiS_2$. The optimum fluorine content of ~24% at O-sites resulted in the composition with maximum $T_c \sim 3.5$ K. In another report [22], high-pressure annealing of the as-synthesized samples was carried out; T_c of such materials is reported to be 5.1 K. We observe a significantly higher $T_c \sim 5.3$ K in our sample of $BiO_{0.75}F_{0.25}BiS_2$. In view of such procedural change in the synthesis of the title material we have carried out detailed studies on this system, including the high-pressure magnetization studies.

2. Experimental

Polycrystalline sample of nominal composition $BiO_{0.75}F_{0.25}BiS_2$ was prepared by the solid-state sealed-tube method. The reactants BiF_3, Bi_2O_3, Bi_2S_3 and Bi metal were weighed and mixed in the stoichiometric ratio in an Ar-filled glove box with O_2 and H_2O content <1 ppm. Bi_2S_3 was pre-synthesized

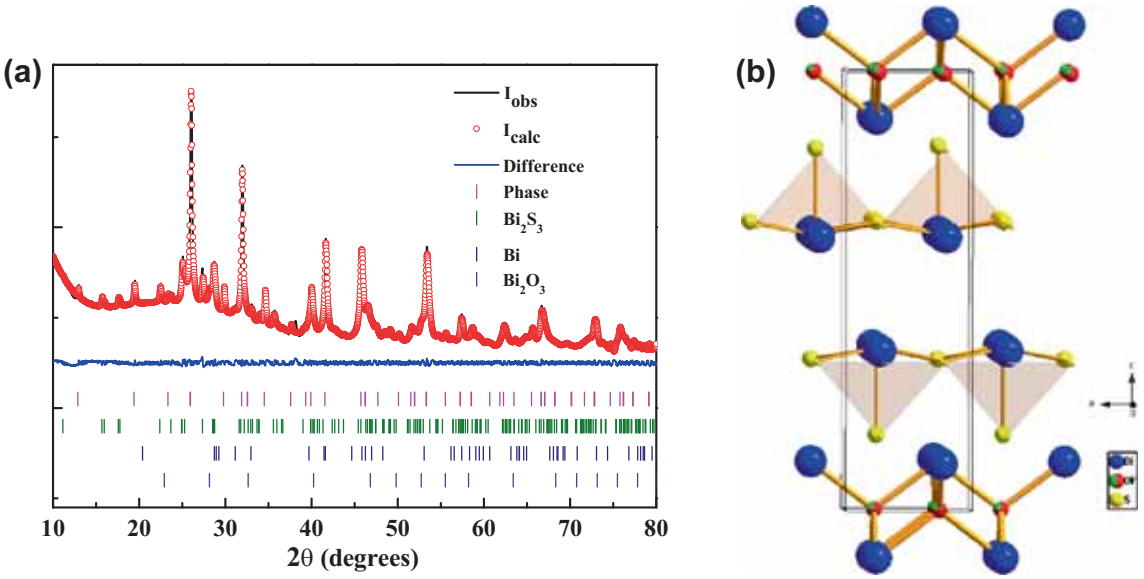

Figure 1. (**a**) Rietveld refinement studies of $BiO_{0.75}F_{0.25}BiS_2$ at room temperature (left) and (**b**) crystal structure of $BiO_{0.75}F_{0.25}BiS_2$ (right).

by the reaction of the elements at 500°C for 15 h in vacuum. The mixture of reactants was pelletized and sealed in an evacuated quartz tube and heated at 430°C for 24 h followed by quenching in ice water. The product so obtained was sintered twice under the same heating condition to improve the phase purity. The product obtained was dark-black in colour and was stable in air. The phase purity of the sample was checked by powder XRD using Cu-Kα radiation and a Bruker D8 advance diffractometer. Rietveld refinement of the powder XRD data was carried out using the *TOPAS* software package [23]. Magnetization of the polycrystalline sample was studied at various applied pressures up to ∼1 GPa in the temperature range 2–300 K in an applied magnetic field of 10 Oe in ZFC mode using a vibrating sample magnetometer (VSM) option in the Physical Property Measurement System (PPMS, Quantum Design, USA). A mixture of Fluorinert FC 70 and FC 77 (1:1) was used as the pressure-transmitting medium. The ambient resistivity measurements in applied magnetic field were carried out in the temperature range 2–300 K using a conventional four-probe method in the PPMS-VSM.

3. Results and discussion

The powder XRD pattern of $BiO_{0.75}F_{0.25}BiS_2$ confirms the formation of a tetragonal $CeOBiS_2$-type phase [24] with space group $P4/nmm$ (#129) as shown in figure 1a. Minor impurity peaks corresponding to Bi_2S_3, Bi_2O_3 and Bi metal (total impurity content $< 15\%$) were detected. The crystal structure of $BiO_{0.75}F_{0.25}BiS_2$, shown in figure 1b, comprises layers of edge-sharing tetrahedral Bi_2O_2 alternating with conducting square pyramidal BiS_2-bilayers. Structural parameters were calculated by Rietveld fit to powder XRD data in the 2θ range 10–80°, results of which are shown in table 1. The determined lattice parameters $a = 3.9663(3)$ Å, $c = 13.730(2)$ Å and the cell volume $V = 215.99(4)$ Å^3 are quite close to those reported previously for $BiO_{0.75}F_{0.25}BiS_2$ [13]. They are smaller than those of the parent $BiOBiS_2$ ($a = 3.9744$ Å, $c = 13.7497$ Å and $V = 220.8$ Å^3) [13]. This decrease in the cell parameters indicates effective doping as the F^{1-} ion is smaller than O^{2-}, showing clearly that F^{1-} has replaced O^{2-} ions. We carried out the compositional analysis of the sample using SEM–EDX. A typical SEM micrograph (figure 2) shows the presence of Bi- and S-element. The actual fractions of oxygen and fluorine could not be estimated by EDX measurements. The ratio of Bi and S elements was $Bi_{2.2}F_{0.26}S_{2.1}$, which is quite close to that of the nominal composition.

The zero-field temperature-dependent resistivity of $BiO_{0.75}F_{0.25}BiS_2$ in the temperature range 2–300 K is shown in figure 3. The room temperature resistivity is about 4 mΩ cm. The sample shows typical metallic conduction, and a sharp superconducting transition with T_c^{onset} at 5.3 K. The criterion of determining onset T_c is shown in the lower left inset of figure 3. The lower right inset of figure 3 shows the field dependence of variable temperature resistivity. At zero magnetic fields the transition width is 1 K, which broadens considerably on applying field. The upper inset of figure 3 shows the H–T phase diagram for $BiO_{0.75}F_{0.25}BiS_2$ corresponding to the temperature where the resistivity is 90 and 10% of the normal state resistivity. As the initial part of the plot does not follow the WHH curve, we do not apply the WHH formula in our case. However, we can infer from our plot that the eventual $H_{c2}(0)$ would certainly be higher than (or equal to) 3 T. The previous report [13] shows that the value of the upper critical field

Table 1. Refined lattice parameters for $BiO_{0.75}F_{0.25}BiS_2$.

Space group	$P4/nmm$
R_{wp}(%)	4.13
χ^2	2.24
$a = b$ (Å)	3.9663(3)
c (Å)	13.730(2)
v (Å^3)	215.99(4)

Atom	Site	x	y	z	Occupancy (fixed)
Bi	2c	0.25	0.25	0.1087(7)	1
O/F	2a	0.75	0.25	0	0.75/0.25
Bi	2c	0.25	0.25	0.6301(1)	1
S1	2c	0.25	0.25	0.353(5)	1
S2	2c	0.25	0.25	0.827(4)	1

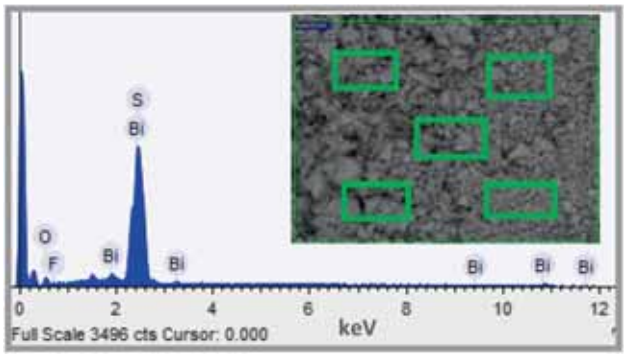

Figure 2. EDAX analysis for $BiO_{0.75}F_{0.25}BiS_2$ showing the presence of all elements. Inset shows the SEM micrograph of the same sample and the highlighted regions, at which the data were collected.

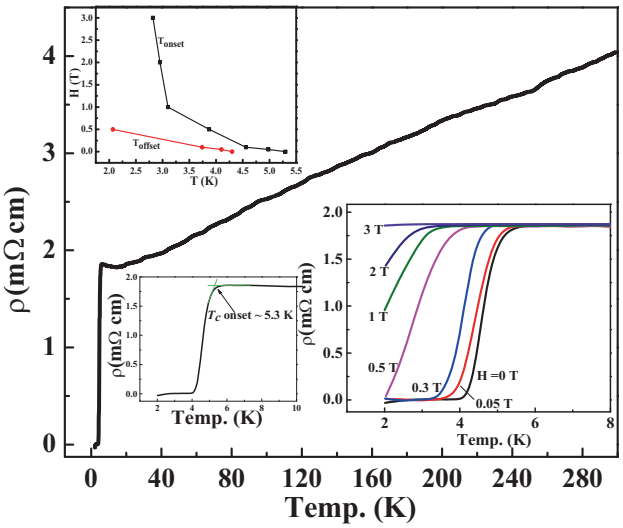

Figure 3. Resistivity *vs.* temperature (ρ–T) behaviour of $BiO_{0.75}F_{0.25}BiS_2$ in zero applied field. The lower left inset shows the criterion of obtaining T_c onset and lower right inset shows temperature dependence of electrical resistivity of $BiO_{0.75}F_{0.25}BiS_2$ in several applied external magnetic fields in the superconducting region. The upper inset shows temperature dependence of upper critical field.

for $BiO_{0.75}F_{0.25}BiS_2$ is 1.95 T. We calculate the Ginzburg–Landau coherence length $\xi = [\Phi_0/(2\pi H_{c2})]^{1/2}$, where Φ_0 is the magnetic flux quantum and its value $\Phi_0 = 2.07 \times 10^{-7}$ G cm^2. The coherence length $\xi_{GL}(0)$ is estimated to be ~ 85 Å for $BiO_{0.75}F_{0.25}BiS_2$, which is lower than the values reported for BiS_2-based material [13,25].

In the $\rho(T, H)$ experiment, along with the lowering of T_c we observe a broadening of the resistive transition on application of external magnetic field. This hints towards active role of thermal fluctuations of vortices in $BiO_{0.75}F_{0.25}BiS_2$. Thus, the movement of vortices is evident and it follows the same model of Arrhenius-type thermally activated behaviour described by the equation $\rho(T, H) = \rho_0 \exp(-U_0/k_BT)$ as discussed in literature [25]. The magnetic field dependence of the activation energy (U_0) is shown in figure 4. The inset of figure 4 shows the Arrhenius plot ($\ln(\rho)$ *vs.* T^{-1}). The inset shows that the electrical resistivity is thermally activated in the region of resistivity between 11 and 16 mΩ cm. The activation energy U_0 is calculated from the slope of the curve in this linear region using the afore-mentioned formula. The best fit to the experimental data yields the values of the activation energy $U_0/k_B \sim 89$ K (0 T) and is suppressed to ~0.031 K (3 T) for $BiO_{0.75}F_{0.25}BiS_2$. The value of activation energy in the absence of field is less than that reported for $Bi_4O_4S_4$ superconductor [25]. The gradual decrease in U_0 with increase in magnetic field (from $H = 0$ to 3 T) for $BiO_{0.75}F_{0.25}BiS_2$ superconductor suggests strong vortex pinning forces in the presence of an applied magnetic field.

The variation of DC magnetization as a function of temperature for $BiO_{0.75}F_{0.25}BiS_2$ is shown in figure 5. Magnetization measurements are carried out near the superconducting transition temperature, for both the field-cooled (FC) and zero-field-cooled (ZFC) modes in an applied field of 20 Oe.

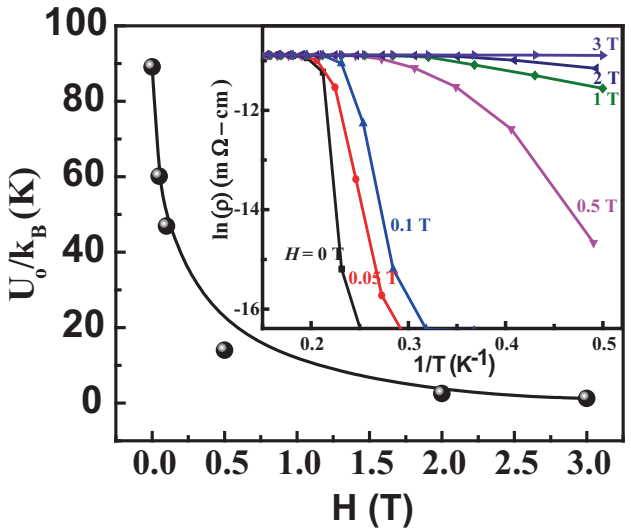

Figure 4. The magnetic field (H) dependence of the activation energy (U_0/k_B). Inset shows Arrhenius plot of $BiO_{0.75}F_{0.25}BiS_2$ at low temperature.

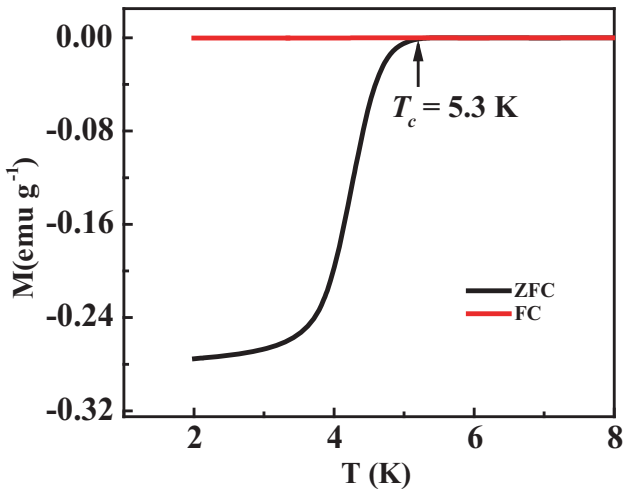

Figure 5. Temperature-dependent DC magnetization at ambient pressure in the FC and ZFC modes for $BiO_{0.75}F_{0.25}BiS_2$ at 20 Oe.

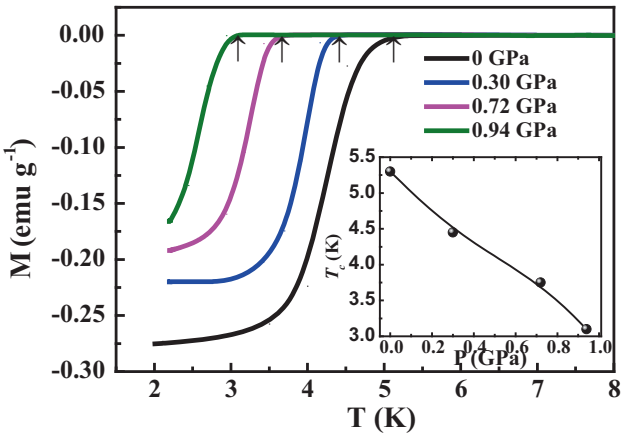

Figure 6. Pressure dependence of DC magnetization as a function of varying temperature at 20 Oe. Inset shows the decrease in T_c on applying external pressure.

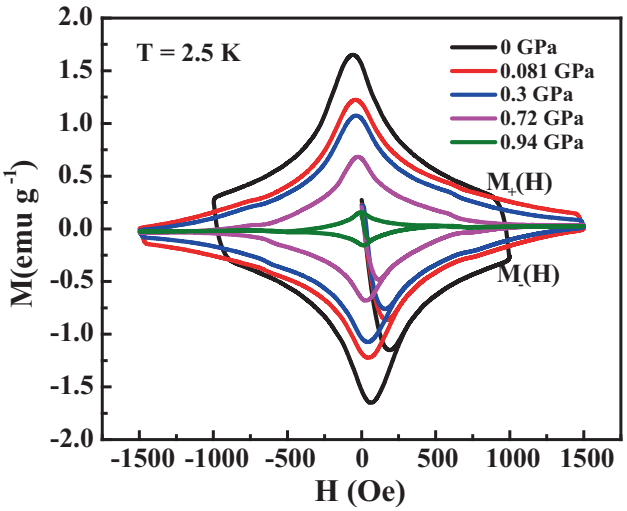

Figure 7. Pressure dependence of isothermal magnetization as a function of applied magnetic field 1500 Oe at 2.5 K. M_+ and M_- are respective values of magnetization at a given field H. $M_+ - M_-$ is a measure of critical current at a field H and at pressure P.

A sharp diamagnetic signal at $T_c^{onset} \sim 5.3$ K is observed. This value matches well with the onset T_c obtained in electrical resistivity measurement. On applying hydrostatic pressure ($0 < P < 1$ GPa), the diamagnetic signal shifts to lower temperature as shown in figure 6. We observe a similar effect of negative pressure dependence of T_c by high-pressure magnetization measurements as seen in high-pressure resistivity studies [22]. In figure 7 we show how the superconducting hysteresis loop of the sample measured in an applied field H, where -1500 Oe $\leq H \leq +1500$ Oe, varies at various values of external pressure. The M–H plot indicates type-II behaviour of the compound, with both H_{c1} and H_{c2} decreasing upon application of pressure. It is clear that the difference $M_+ - M_-$ at any given field decreases with the increase of pressure, implying that the critical current decreases as a function of applied pressure. We show in figure 8 the pressure effects on magnetic-field-dependent critical current density at 2.5 K. The critical current density J_c at different pressures was calculated from the $M(H)$ plot as shown in figure 8. We used the Beans model [26], according to which $J_c = 20\Delta M/d$, where ΔM is the difference between the increasing and decreasing branch of magnetization at an applied field value and d is the average grain size. Based on the afore-mentioned observation we tabulate our results showing decrease in T_c and J_c on applying pressure in $BiO_{0.75}F_{0.25}BiS_2$.

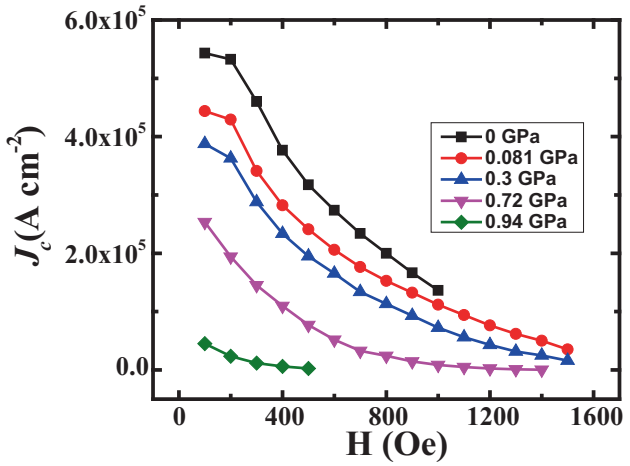

Figure 8. Magnetic field dependence of critical current density (J_c) measured at 2.5 K in the presence of applied pressures $0 \leq P \leq 0.94$ GPa.

Pressure (GPa)	T_c (K) from M–T plot	J_c (A cm^{-2}) at 100 Oe
0	5.3	5.4×10^5
0.081	4.97	4.4×10^5
0.3	4.45	3.9×10^5
0.72	3.75	2.5×10^5
0.94	3.1	4.5×10^4

4. Conclusions

We obtained a superconducting transition temperature (T_c) = 5.3 K for $BiO_{0.75}F_{0.25}BiS_2$ from resistivity measurements. The pressure-dependent magnetization measurements show decrease in T_c, which is consistent with earlier reports. We have measured the superconducting hysteresis loop as a function of magnetic field under various pressures and the upper critical field in $BiO_{0.75}F_{0.25}BiS_2$ is found to be higher than the earlier report on this material. There is a gradual decrease in activation energy U_0/k_B with increase in magnetic field (from $H = 0$ to 3 T) for $BiO_{0.75}F_{0.25}BiS_2$. We observe a decrease in J_c and T_c under applied external pressure.

Acknowledgements

AKG thanks DST for providing financial support. ZH and GST thank UGC and CSIR, respectively, for a fellowship. GKS and SA acknowledge the DST, DRDO, BRNS and UGC (RFSMS-SRF-Meritorious fellowship) for their financial support.

References

[1] Yazici D, Huang K, White B D, Chang A H, Friedman A J and Maple M B 2013 *Philos. Mag.* **93** 673
[2] Mizuguchi Y, Demura S, Deguchi K, Takano Y, Fujihisa H, Gotoh Y *et al* 2012 *J. Phys. Soc. Jpn.* **81** 114725
[3] Nagao M, Demura S, Deguchi K, Miura A, Watauchi S, Takei T *et al* 2013 *J. Phys. Soc. Jpn.* **82** 113701
[4] Jha R, Kumar A, Singh S K and Awana V P S 2013 *J. Supercond. Nov. Magn.* **26** 499
[5] Xing J, Li S, Ding X, Yang H and Wen H H 2012 *Phys. Rev. B* **86** 214518
[6] Jha R, Kumar A, Singh S K and Awana V P S 2013 *J. Appl. Phys.* **113** 056102
[7] Yazici D, Huang K, White B D, Jeon I, Burnett V W, Friedman A J *et al* 2013 *Phys. Rev. B* **87** 174512
[8] Demura S, Mizuguchi Y, Deguchi K, Okazaki H, Hara H, Watanabe T *et al* 2013 *J. Phys. Soc.* **82** 033708
[9] Lin X, Ni X, Chen B, Xu X, Yang X, Dai J *et al* 2013 *Phys. Rev. B* **87** 020504(R)
[10] Lei H, Wang K, Abeykoon M, Bozin E S and Petrovic C 2013 *Inorg. Chem.* **52** 10685
[11] Thakur G S, Fuchs G, Nenkov K, Haque Z, Gupta L C and Ganguli A K 2016 *Sci. Rep.* **6** 37527
[12] Jha R, Tiwari B and Awana V P S 2015 *J. Appl. Phys.* **117** 013901
[13] Shao J, Yao X, Liu Z, Pi L, Tan S, Zhang C *et al* 2015 *Supercond. Sci. Technol.* **28** 015008
[14] Zhai H F, Zhang P, Tang Z T, Bao J K, Jiang H, Feng C M *et al* 2015 *J. Phys.: Condens. Matter* **27** 385701
[15] Thakur G S, Jha R, Haque Z, Awana V P S, Gupta L C and Ganguli A K 2015 *Supercond. Sci. Technol.* **28** 115010
[16] Wolowiec C T, White B D, Jeon I, Yazici D, Huang K and Maple M B 2013 *J. Phys.: Condens. Matter* **25** 422201
[17] Wolowiec C T, Yazici D, White B D, Huang K and Maple M B 2013 *Phys. Rev. B* **88** 064503
[18] Tomita T, Ebata M, Soeda H, Takahashi H, Fujihisa H, Gotoh Y *et al* 2014 *J. Phys. Soc. Jpn.* **83** 063704
[19] Jha R, Tiwari B and Awana V P S 2014 *J. Phys. Soc. Jpn.* **80** 063707
[20] Mizuguchi Y, Fujihisa H, Gotoh Y, Suzuki K, Usui H, Kuroki K *et al* 2014 *Phys. Rev. B* **90** 220510
[21] Kotegawa H, Tomita Y, Tou H, Izawa H, Mizughchi Y, Miura O *et al* 2012 *J. Phys. Soc. Jpn.* **81** 103702
[22] Okada T, Ogino H, Shimoyama J-I, Kishio K, Takeshita N, Shirakawa N *et al* 2015 *J. Phys. Soc. Jpn.* **84** 1
[23] Bruker A X S GmbH 2009 *TOPAS V4.2: general profile and structure analysis software for powder diffraction data*
[24] Céolin R and Rodier N 1976 *Acta Crystallogr. B* **32** 1476
[25] Srivastava P, Shruti and Patnaik S 2014 *Supercond. Sci. Technol.* **27** 055001
[26] Bean C P 1964 *Rev. Mod. Phys.* **36** 31